*Polymorphism in a common Atlantic reef coral (*Montastraea cavernosa*) and its long-term evolutionary implications*

Ann F. Budd, Flavia L. D. Nunes, Ernesto Weil & John M. Pandolfi

Evolutionary Ecology

ISSN 0269-7653
Volume 26
Number 2

Evol Ecol (2012) 26:265-290
DOI 10.1007/s10682-010-9460-8

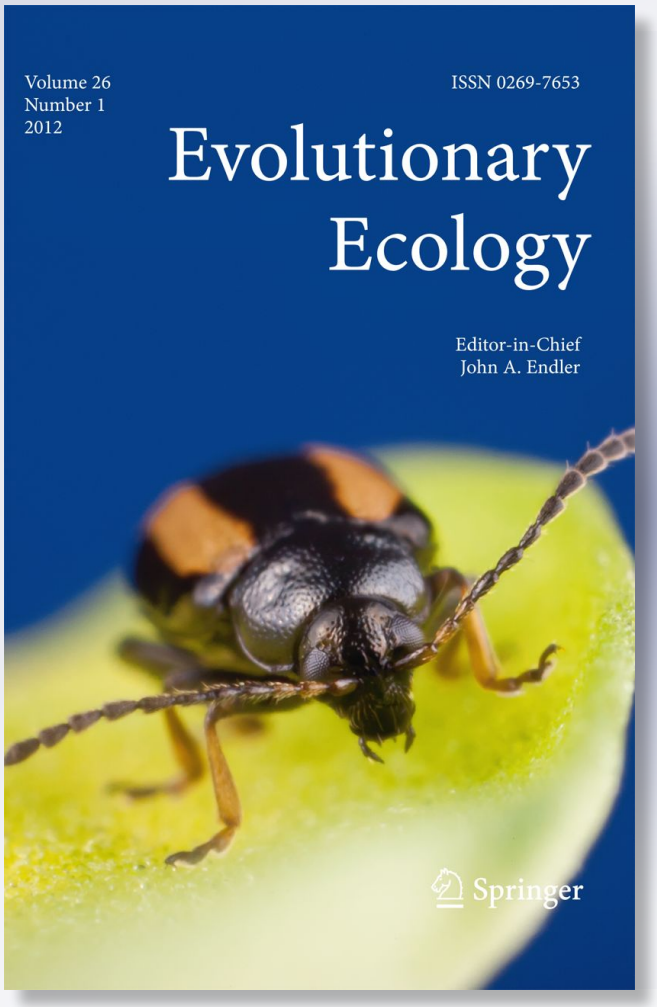

Springer

Evol Ecol (2012) 26:265–290
DOI 10.1007/s10682-010-9460-8

ORIGINAL PAPER

Polymorphism in a common Atlantic reef coral (*Montastraea cavernosa*) and its long-term evolutionary implications

Ann F. Budd · Flavia L. D. Nunes · Ernesto Weil · John M. Pandolfi

Received: 21 September 2010 / Accepted: 23 December 2010 / Published online: 20 January 2011

Abstract Recent advances in morphometrics and genetics have led to the discovery of numerous cryptic species in coral reef ecosystems. A prime example is the *Montastraea annularis* scleractinian coral species complex, in which morphological, genetic, and reproductive data concur on species boundaries, allowing evaluation of long-term patterns of speciation and evolutionary innovation. Here we test for cryptic species in the Atlantic species, *Montastraea cavernosa*, long recognized as polymorphic. Our modern samples consist of 94 colonies collected at four locations (Belize, Panamá, Puerto Rico in the Caribbean; São Tomé in the Eastern Atlantic). Our fossil samples consist of 78 colonies from the Plio-Pleistocene of Costa Rica and Panamá. Landmark morphometric data were collected on thin sections of 46 modern and 78 fossil colonies. Mahalanobis distances between colonies were calculated using Bookstein coordinates, revealing two modern and four fossil morphotypes. The remaining 48 of the 94 modern colonies were assigned to morphotype using discriminant analysis of calical measurements. Cross-tabulation and multiple comparisons tests show no significant morphological differences among

Electronic supplementary material The online version of this article (doi:10.1007/s10682-010-9460-8) contains supplementary material, which is available to authorized users.

A. F. Budd (✉)
Department of Geoscience, University of Iowa, Iowa City, IA 52242, USA
e-mail: ann-budd@uiowa.edu

F. L. D. Nunes
Center for Marine Biodiversity and Conservation, Scripps Institute of Oceanography, La Jolla, CA 92093, USA

F. L. D. Nunes
Observatoire des Sciences de l'Univers de Rennes, Université de Rennes 1, 35069 Rennes, France

E. Weil
Department of Marine Sciences, University of Puerto Rico, Mayagüez, PR 00681, USA

J. M. Pandolfi
Centre for Marine Science, School of Biological Sciences, and Australian Research Council Centre of Excellence for Coral Reef Studies, The University of Queensland, Brisbane, QLD 4072, Australia

geographic locations or water depths. Patterns of variation within and among fossil morphotypes are similar to modern morphotypes. DNA sequence data were collected for two polymorphic nuclear loci *(β-tub1* and *β-tub2*) on all 94 modern colonies. Haplotype networks show that both genes consist of two clades, but morphotypes are not associated with genetic clades. Genotype frequencies and two-locus genotype assignments indicate genetic exchange across clades, and ϕst values show no genetic differentiation between morphotypes at different locations. Taken together, our morphological and genetic results do not provide evidence for cryptic species in *M. cavernosa*, but indicate instead that this species has an unusually high degree of polymorphism over a wide geographic area and persisting for >25 million years (myr).

Keywords Cryptic species · Reef coral · Caribbean · Geometric morphometrics · *β-tubulin* · Neogene

Introduction

Evolutionary theory predicts that gene flow between large established populations of demographically stable species prevents natural selection and genetic drift from causing population differentiation (Slatkin 1987). Gene flow thus acts as a constraining force to speciation. Over geologic time, species with large population sizes and wide geographic distributions are expected not only to have low speciation rates but also to have long species durations and be better able to survive environmental perturbations associated with mass extinctions (Jablonski 2007 and references therein). The fossil record provides the only source of long-term data (>100 K years) for studying speciation, extinction, and the evolution of species lineages, and thus for testing relationships between spatial and temporal parameters including speciation rate and species duration. However, study of species in the fossil record assumes that morphologically recognized species correspond with biological species. Jackson and Cheetham (1990, 1999) were among the first to test this correspondence, and demonstrate concordance between morphospecies and genetically delineated ones, clearly showing punctuated speciation and stasis in bryozoans and supporting the theory of punctuated equilibrium (Eldredge and Gould 1972). Combined analyses of morphological, genetic, and reproductive data have also been applied to various marine organisms on modern coral reefs, revealing large numbers of previously undiscovered cryptic species (Knowlton 1993, 2000; Knowlton and Jackson 1994; Klautau et al. 1999; Lee and Foighil 2005; Mathews 2006; Calvo et al. 2009; Lin et al. 2009; Barroso et al. 2010) and underscoring the fact that current understanding of the speciation process in these organisms is inadequate. Here we examine the relationship between population size, geographic distribution, speciation rate, and species duration in a common reef coral, in an effort to better predict how this currently endangered group of organisms (Carpenter et al. 2008) will respond to the many environmental factors, ranging from local to global in scale, which are increasingly threatening coral reefs.

Previous work on speciation in reef corals (Knowlton et al. 1992; Weil and Knowlton 1994; Fukami et al. 2004a; Budd and Pandolfi 2004, 2010), specifically the *Montastraea annularis* species complex, has combined not only morphological, genetic, reproductive, and fossil data but also added a geographic component, and found that most evolutionary innovation and speciation occurs at the edge of species distributions. However, genetic analyses of other species suggest that this geographic pattern may not be the case in all reef corals. For example, Nunes et al. (2009) discovered lower levels of genetic diversity in

peripheral populations of *Montastraea cavernosa* in Brazil and West Africa than in central populations in the Caribbean. At the species level, however, *M. cavernosa* exhibits a high level of genetic variation in two copies of the *β-tubulin* gene *(β-tub1* and *β-tub2*), and both loci are characterized by the presence of two clades of haplotypes (Nunes et al. 2009). The divergence between these two clades exceeds the level of intra-specific divergence observed for this gene in other species (Nunes et al. 2008), and could be an indication of the presence of cryptic species.

In the present paper, we investigate possible cryptic species in *M. cavernosa* by further exploring patterns of spatial and temporal variation. Specifically we test for correspondence between morphological and genetic data, and compare patterns observed today with those in the fossil record. Our analyses of morphology are based on a geometric morphometric approach, which has been shown to be more effective than traditional morphological features at distinguishing cryptic species in the *M. annularis* species complex (Knowlton and Budd 2001; Budd and Klaus 2001). Our genetic analyses use published DNA sequences from two polymorphic nuclear loci *(β-tub1* and *β-tub2*) (Nunes et al. 2009). Our fossil analyses are based on large, well-dated collections ranging in age from the late Pliocene to early Pleistocene of Costa Rica and Panamá (Budd et al. 1999), sampled in collaboration with the Panamá Paleontology Project (Collins and Coates 1999).

We address the following questions:

1. Can distinct morphotypes be recognized in modern *M. cavernosa*?
2. If so, are these morphotypes genetically distinct and do they represent cryptic species?
3. Is the observed morphological and genetic variation related to either geography or environment?
4. Are the many morphospecies of *M. cavernosa*-like corals reported in the Cenozoic Caribbean fossil record as distinct as the morphotypes observed today? Could they represent separate biological species?
5. How do studies integrating morphological, genetic, and fossil data contribute to understanding the long-term evolution of *M. cavernosa*?

Our results show that, in contrast to the *M. annularis* species complex, *M. cavernosa* does not contain cryptic species, but instead shows high degrees of both morphological and genetic polymorphism, which are not concordant and are unrelated to geography and environment. This high degree of polymorphism has been a persistent characteristic of *M. cavernosa* since at least the late Pliocene, perhaps even as far back as the late Oligocene, and may be responsible for its unusually long species duration.

We dedicate this article to Jeremy B. C. Jackson and Alan H. Cheetham, whose pioneering empirical work on morphological stasis and speciation in colonial marine organisms paved the way for the present study.

Materials and methods

Species studied

The reef coral *Montastraea cavernosa* (Linneaus 1767) is a common, widely distributed species, whose water depth distribution extends from 0.5 to 95 m, with highest occurrences in intermediate to deep reef depths of 10–60 m (Goreau 1959; Goreau and Wells 1967). Its geographic distribution extends across the Caribbean, as far north as Bermuda in the North Atlantic, and to Brazil in the South Atlantic and the Gulf of Guinea in the Eastern Atlantic

(Laborel 1969, 1974; Sterrer 1986). Like members of the *Montastraea annularis* species complex, *M. cavernosa* is characterized by massive colonies with discrete corallites, which have well-developed costae and coenosteum and trabecular columellae (Budd 1991). However, molecular data indicate that the *M. annularis* complex and *M. cavernosa* are phylogenetically divergent and should be placed in separate genera (Fukami et al. 2004b, 2008). Moreover, molecular trees (Fukami et al. 2004b, 2008) show that *M. cavernosa* is basal to almost all other Atlantic and Indo-Pacific faviid corals, and studies of the fossil record suggest that the species extends back as far as the late Oligocene (Johnson 2007), with similar species (e.g., *Montastraea nodosa*) occurring in the middle Eocene (Budd et al. 1992).

M. cavernosa is a gonochoric broadcast spawning species with an annual cycle of gametogenesis (Szmant 1991; Szmant et al. 1996). Spawning occurs approximately one week after the full moon in August and September (Acosta and Zea 1997). *M. cavernosa* produces larger eggs than the *M. annularis* complex, which may increase larval survival time, dispersal capability, and survivorship after settlement.

Previous ecological studies (Lasker 1976, 1979, 1980, 1981; Budd 1993) have recognized two distinct feeding morphs of *M. cavernosa*: a "diurnal" morph with smaller polyps (5.88 ± 0.81 mm), which are expanded both day and night, and a "nocturnal" morph with larger polyps (7.28 ± 0.94 mm), which are only expanded at night and more effective at capturing zooplankton. The two morphs have been observed occurring side by side, often touching each other (without aggressive behavior) at different depths along the reef profile at many geographic localities around the Caribbean (Fig. 1). A previous multivariate study further exploring the ecological, morphological and behavioral differences between the diurnal and nocturnal morphs of *M. cavernosa* in Puerto Rico (Ruiz 2004) showed that both morphs were abundant across the reef profile but their relative frequencies differed in water depth. Up to 90% of shallow (3–10 m) colonies were the diurnal morph, and 60% of deep (15–25 m) colonies were the nocturnal morph. Colony and/or oral disc coloration varied within and between morphs with the diurnal morph being usually brownish, grayish or pale green, and the nocturnal morph having brighter colors such as orange, red or olive-green. Up to 43% of diurnal-morph colonies had bright green oral discs. Colonies of the diurnal morph were significantly (t test, $P < 0.001$) smaller (with an average surface area of 826.6 ± 3.6 cm^2) than those of the nocturnal morph ($1{,}158.5 \pm 3.9$ cm^2). High variability in colony- and corallite-level characters along the depth gradient was found within each morph, indicating the influence of environment on morphology. However, significant morphological differences between the diurnal and nocturnal morphs were found in at least 8 of 10 calical characters analyzed (from each of 10 corallites in each of 15 colonies of each morph collected from two reefs off La Parguera, $n = 60$). Two distinct groups (diurnal and nocturnal) were clearly separated by canonical discriminant analysis (94.0% of all colonies correctly classified, with corallite diameter and length of the primary septa being most heavily weighted), suggesting a potential cryptic species (Ruiz 2004). The two morphs also differ in geographic distribution with the diurnal morph being dominant in Bermuda (Weil, pers. observ.).

Similarly, studies of the Plio-Pleistocene Caribbean fossil record indicate that numbers of *M. cavernosa*-like morphotypes range from five (Budd 1991) to seven (Vaughan 1919) to eight (Schultz and Budd 2008), which differ in corallite size, number of septa per corallite, the relative development of different costal cycles, and corallite wall structure. The present study examines whether all of these morphotypes, both modern and fossil, could be cryptic species.

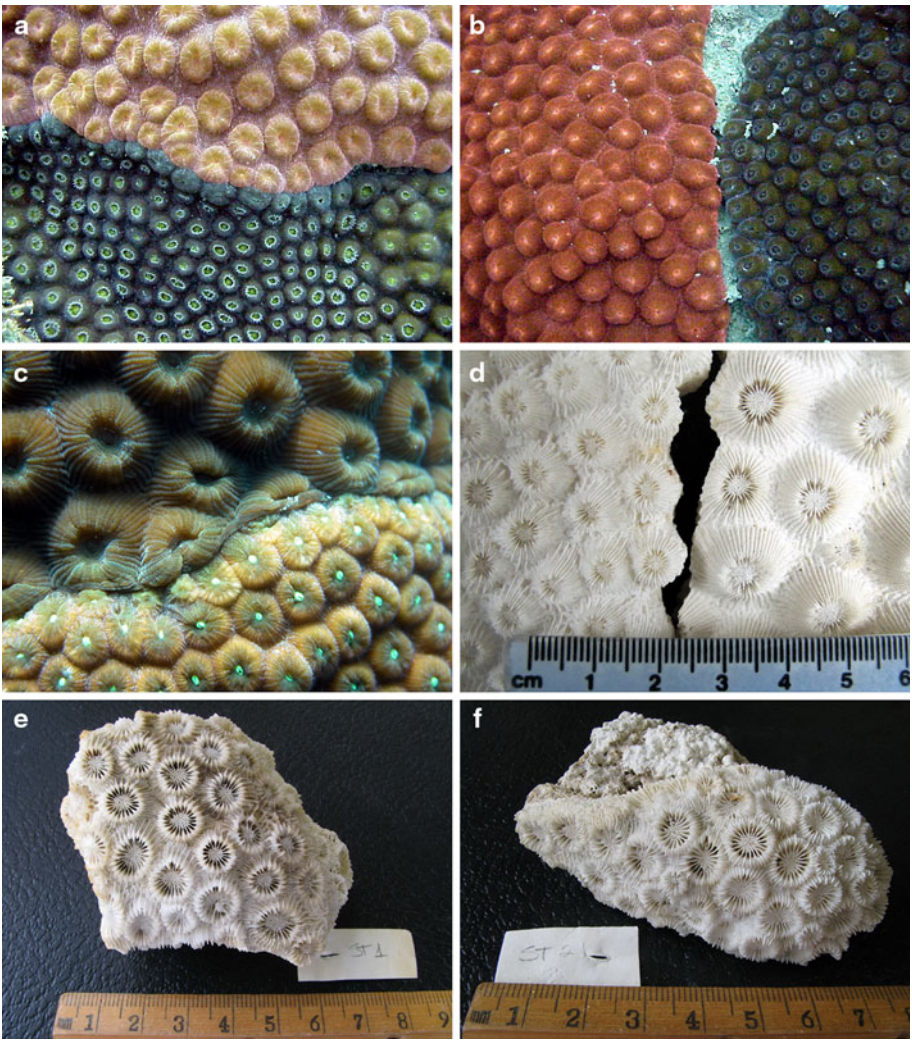

Fig. 1 Photographs of colonies of the two morphs of *M. cavernosa* growing side-by-side in reefs off Puerto Rico (**a**–**d**) showing active (expanded tentacles) small-polyped diurnal colonies and inactive large-polyped nocturnal colonies and the coloration differences (**a**–**c**), the lack of aggressive behavior (histocompatibility) between touching colonies (**a** and **c**) and the significant difference in polyp size, intercalice distances, and number of calices/area. Photographs of the two morphs collected in São Tomé (**e**, small-polyped; **f**, large-polped) showed less distinctive differences, and the more intergradational nature of morphological variation. Photos **a**–**d**, E. Weil; **e**–**f**, F. Nunes

Sampling

A total of 94 modern colonies of *Montastraea cavernosa* were collected and characterized both morphologically and genetically from four geographic locations: Belize (39 colonies), Panamá (6 colonies), and Puerto Rico (23 colonies) in the Caribbean; and the Island of São Tomé in the Republic of São Tomé & Príncipe (26 colonies) in the Eastern Atlantic

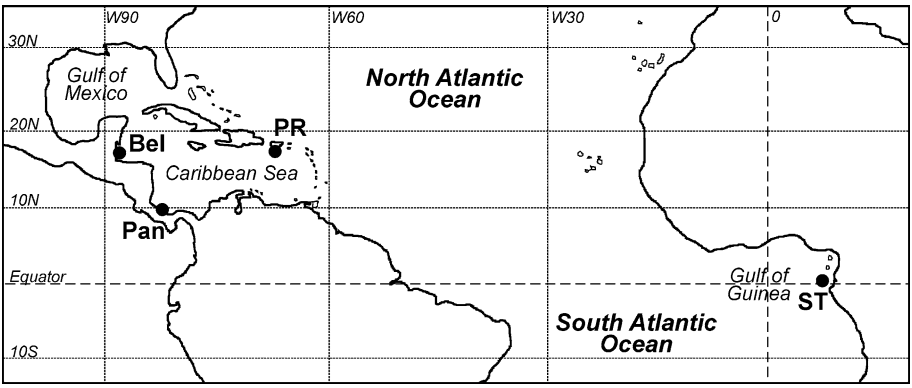

Fig. 2 Locality map showing the four geographic locations where modern corals were collected. *Bel* Belize, *Pan* Panamá, *PR* Puerto Rico, *ST* São Tomé. Belize colonies were collected at Carrie Bow Cay reef at depths of 5–22 m (Supplemental Table S1). Panamá colonies were collected at Hospital Point, Bocas del Toro, at a maximum depth of 9 m (31 ft). Puerto Rico colonies were collected at depths of 4–20 m from the Parguera area and other localities along the west coast (Desecheo island). São Tomé colonies were collected at depths of 7–23 m

(Fig. 2). A range of environments and depths was sampled at each location. Hammer and chisel were used to break off a piece of the colony that contained at least 10 corallites for morphological analysis. Fresh coral tissue from the same samples was preserved in guanidine thiocyanate solution (4 M guanidine thiocyanate, 0.1% N-lauroyl sarcosin sodium, 10 mM Tris pH8, 0.1 M 2-mercaptoethanol) and was kept at room temperature until DNA could be extracted. Skeletons were submerged in household bleach for approximately 24–48 h, rinsed in fresh water for another 24 h and left to dry in the sun for 24 h. A complete list of modern coral samples is given in Supplemental Table S1. Skeletons from Belize, Panamá, and São Tomé are deposited in the Paleontology Repository of the University of Iowa (SUI); skeletons from Puerto Rico are deposited at the Department of Marine Sciences, University of Puerto Rico, Mayagüez, PR.

A total of 78 fossil colonies of *M. cavernosa*-like corals with >36 septa per corallite (Supplemental Table S2) were collected and morphologically characterized from the Moín Formation near Limón, Costa Rica (47 colonies) and the La Gruta Formation on the islands of Colón and Bastimentos including Wild Cane Key, in the Bocas del Toro region of Panamá (31 colonies). Colonies from the Moín Formation are dated at 2.9–1.5 Ma (McNeill et al. 2000); colonies from the La Gruta Formation are dated as 3.5–1.5 Ma (Coates et al. 2005). All fossil colonies are deposited in the Paleontology Repository of the University of Iowa.

Morphological data and analyses

Two morphological datasets were constructed using the modern colonies: (1) linear distance measurements and counts on calical surfaces of all 94 colonies using a stereomicroscope (the "calical surface" dataset), and (2) landmark data on transverse thin sections (30 microns thick) on a subset of 46 colonies using a transmitted light microscope (the "thin section" dataset). Calical surfaces are worn on the fossil colonies; therefore, only a thin section dataset was constructed for fossil colonies.

Modern calical surface dataset

We measured the following linear distances to the nearest tenth of a millimeter and made the following counts on 2–10 corallites per colony (median = 6): maximum corallite diameter, minimum corallite diameter, columella width, primary septum length, total number of septa (see Budd 1991 for measurement definitions). These measurements were used to construct a dataset, which consisted of colony averages for nine variables: (1) maximum corallite diameter [CD-MAX], (2) minimum corallite diameter [CD-MIN], (3) average corallite diameter [CD-AV, calculated using the average of (1) and (2)], (4) columella width [CW], (5) the ratio between columella width and average corallite diameter [CW-RAT], (6) primary septum length [SL], (7) the ratio between primary septum length and average corallite diameter [SL-RAT], (8) the ratio between minimum and maximum corallite diameter [ROUNDNESS], and (9) total number of septa [NOSEPTA].

Modern thin section dataset

We digitized the Cartesian coordinates (x–y) of 21 landmarks to the nearest hundredth of a millimeter on six corallites per colony (Fig. 3; Supplemental Table S3). Size and shape coordinates (Bookstein 1991; Zelditch et al. 2004) were calculated for the landmark data using the computer program CoordGen6 in the IMP software series (Integrated Morphometrics Package, 2004, written by H. David Sheets, available at http://www2.canisius.edu/~sheets/morphsoft.html). Centroid size is a measure of overall corallite size, and was calculated by summing the squared distances from each of the 21 landmarks to a common centroid. Shape coordinates are size-independent variables, and were calculated for triplets of points in which points 8 and 16 were fixed as the baseline. X-coordinates are ratios of distances along the baseline relative to the length of the baseline; y-coordinates are ratios of point-to-baseline distances relative to the length of the baseline. To facilitate morphological interpretation, 11 shape coordinates associated with the structure and development of the corallite wall and costosepta (Table 1) were selected for use in statistical analyses.

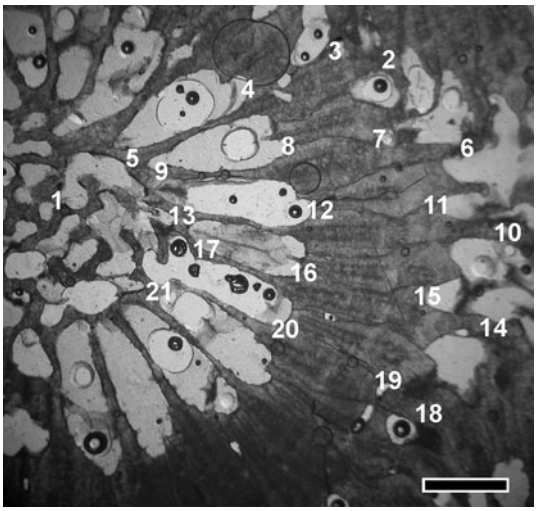

Fig. 3 Two-dimensional Cartesian coordinates collected for 21 landmarks on transverse thin sections of corallites. The landmarks characterize the structure of the corallite wall and costal extensions beyond the wall. Point numbers 8 and 16 were used as the baseline when calculating Bookstein shape coordinates. Specimen E13-5 (SUI 108553), M1, scale bar = 1 mm

Table 1 List of variables in the thin section dataset, consisting of 11 shape coordinates (x12, y1…y17), centroid size (csize), and number of septa

Variables	Related morphological feature	Tukey's HSD multiple comparisons test (homogeneous subsets [in brackets] for $P < 0.05$)
y1	Corallite diameter	[F2 = M2 = F3 = M1] < [M2 = F3 = M1 = F4 = F1]
y6	Extension of tertiary costa (−)	[F4 = F3] < [F3 = F2 = F1] < [F2 = F1 = M1 = M2]
y7	Wall thickness (−)	F4 < [F3 = M1] < [M1 = M2 = F1 = F2]
y9	Tertiary septum length	[F4 = F3] < [F3 = 2=M2] < [F2 = M2 = M1] < [M1 = F1]
y10	Extension of secondary costa (−)	[F4 = F3] < [F3 = F2 = F1] < [F2 = F1 = M1] < [F1 = M1 = M2]
y11	Wall thickness (−)	F4 < [F3 = M1] < [M1 = M2 = F1 = F2]
x12	Relative thickness of secondary and tertiary costa	[M2 = F3 = F1 = M1 = F2] < [F3 = F1 = M1 = F2 = F4]
y13	Secondary septum length	[F4 = F3 = F2 = M2] < [F3 = 2=M2 = M1] < F1
y14	Extension of tertiary costa (−)	[F4 = F3] < [F3 = F2 = F1] < [F2 = F1 = M1 = M2]
y15	Wall thickness (−)	F4 < [F3 = M1] < [M1 = M2 = F1 = F2]
y17	Tertiary septum length	[F4 = 2] < [F2 = F3 = M2] < [F3 = M2 = M1] < [M1 = F1]
csize	Centroid size (all 21 landmarks)	M2 < [F2 = M1 = F3] < [M1 = F3 = F1] < F4
Number of septa	Count of the total number of septa per corallite	[F2 = M2 = M1 = F3 = F1] < [M1 = F3 = F1 = F4]

Values for all shape coordinates are relative to baseline length (i.e., the distance between points 8 and 16). X-coordinates parallel the baseline; y-coordinates are distances from the baseline. Centroid size is a measure of overall corallite size (see text for calculation). Modern morphotypes are underlined; and *M* modern; *F* fossil

Statistical analyses

To recognize morphotypes in the modern samples, following the methods in Budd and Klaus (2008), we first performed a canonical discriminant analysis using the thin section dataset (13 variables, consisting of 11 shape coordinates, centroid size, and number of septa) with the 46 colonies assigned as a priori groups. This step resulted in a 46 × 46 matrix of F values derived from Mahalanobis distances, which we input into an average linkage cluster analysis. We then used cross-validated classification results from a second set of pairwise between-cluster canonical discriminant analyses based on the thin section dataset (colony means) to evaluate branching points in the dendrogram and determine a cutoff distance for distinguishing morphotypes. To assign the remaining 48 of the 94 colonies to morphotype (i.e., the colonies that were characterized molecularly but were not thin-sectioned), we performed a third canonical discriminant analysis using the calical surface dataset and the dendrogram morphotypes as a priori groups.

Univariate differences among morphotypes were further assessed for both datasets using multiple comparisons tests, specifically Tukey's honestly significant difference or HSD. Tukey's HSD uses the Studentized range statistic to make all pairwise comparisons among groups. To evaluate geographic and environmental variation and the possible role of phenotypic plasticity, colonies collected at four different locations (Panamá, São Tomé, Belize, Puerto Rico) and at three different water depths in Belize (<10 m, 10–20 m, >20 m) were

compared using crosstabulation statistics (Pearson's Chi-square); and canonical variate (CV) scores were compared among localities and water depths using Tukey's HSD and non-parametric statistics. Statistical analyses were performed using SPSS 17.0 and SAS 9.1.

Fossil thin section dataset and analyses

We prepared transverse thin sections of the fossil colonies using the same methods as the modern colonies, and digitized the Cartesian coordinates of the same 21 landmarks (Fig. 3; Supplemental Table S3) on six corallites per colony. Centroid size and Bookstein shape coordinates were calculated using the same baseline as the modern colonies, and the same 13 variables were analyzed using canonical discriminant analysis with the 78 fossil colonies assigned as a priori groups. The resulting 78 × 78 Mahalanobis distance matrix was input into an average linkage cluster analysis, and the dendrogram was used to recognize four fossil morphotypes as described above for the modern colonies (F1 = 15 colonies, F2 = 9 colonies, F3 = 38 colonies, F4 = 3 colonies, unassigned = 13 colonies). The 13 unassigned fossil colonies were assigned to a fossil morphotype using the classification results of a canonical discriminant analysis in which the fossil morphotypes served as a priori groups.

To compare patterns of variation between the fossil and modern thin section datasets, the two datasets were combined, and a final canonical discriminant analysis was performed using six morphotypes (2 modern, 4 fossil) as a priori groups. Mahalanobis distances between pairwise combinations of the six morphotypes were used to assess differences among morphotypes.

Molecular data and analyses

DNA extraction, amplification and sequencing

The DNA sequences used in this study are a subset of data published in Nunes et al. (2009), from individuals for which morphological measurements could be obtained. Briefly, DNA was extracted using phenol:chroloform as described in Nunes et al. (2008). The nuclear gene *β-tubulin* was amplified by polymerase chain reaction (PCR) using published primers (Fukami et al. 2004a) according to the protocol for the Sigma Taq polymerase kit (Sigma–Aldrich). The thermal cycling conditions included an initial denaturation step at 94°C for 2 min, followed by 35 cycles of 94°C/45 s, 50°C/45 s and 72°C/1 min 30 s, with a final extension step at 72°C for 5 min. In *M. cavernosa*, the *β-tubulin* gene contains a duplication, where two copies of the gene have identical amino acid sequences, but the introns differ in size by 327 bp (Nunes et al. 2009). The long copy of the gene is ~1,000 bp long, and is referred to as *β-tub1*, while the short copy is ~ 700 bp long, and is referred to as *β-tub2*. The two duplications were separated by electrophoresis of the PCR products on a low melt agarose gel, followed by excision and purification of the two bands using the Qiaquick Gel Extraction kit (Qiagen, Valencia, CA). Purified PCR products were sequenced directly on an ABI Sequencer, using the BigDye Terminator v3.1 cycle sequencing chemistry. Each sample was sequenced in the forward and reverse direction.

Sequence data analysis

DNA sequences were obtained for two loci for 94 colonies ($n = 188$ sequences per locus). Genbank accession numbers are listed in Supplemental Table S4. Sequence chromatograms

were viewed and edited using Sequencher v4.5 (Gene Codes Corp.). Heterozygous bases were identified as double peaks in both forward and reverse directions. Six indels were found in the intron of *β-tub1* and one indel in the intron of *β-tub2*. For individuals heterozygous for >2 indels, an internal sequencing primer was used to obtain sequence data between indels (Nunes et al. 2009). In addition, six individuals were cloned using the pGEM-T Vector system (Promega) to obtain full sequences across the introns. For heterozygous individuals, haplotype reconstruction was achieved bioinformatically with the program PHASE v2.1.1 (Stephens and Scheet 2005; Stephens et al. 2001). Sequence data from homozygous individuals and from cloned sequences were used to estimate the best pair of haplotypes for each heterozygous individual. A complete description of parameters used for heterozygous haplotype reconstruction, and for the treatment of indels and excluded sites (total excluded sites = 9 for *β-tub1*; none for *β-tub2*) is given in Nunes et al. (2009).

A statistical parsimony network was constructed for each locus using TCS v1.21 (Clement et al. 2000) after sequences had been aligned using Clustal X v1.83.1 (Thompson et al. 1997). Shading was used to indicate the haplotypes observed in each morphotype. Phylogenetic trees were inferred for each locus using neighbor-joining (NJ) and maximum parsimony methods (MP), implemented in MEGA (Tamura et al. 2007). The evolutionary distances for the NJ tree were computed using the maximum composite likelihood method with 500 bootstrap replicates. The MP tree was obtained using the close-neighbor-interchange algorithm, search level 3, with 10 random addition of sequences and 500 bootstrap replicates. Haplotype frequencies and population differentiation (ϕ_{st}) were calculated with Arlequin v.3.1 (Excoffier et al. 2005), as was linkage disequilibrium among all polymorphic sites on both loci. To calculate the genetic distance between haplotype clades, identical sequences were collapsed into one unique sequence, and each unique sequence was identified by Clade according to its position in the haplotype network. Pairwise distances were calculated with DAMBE (Xia and Xie 2001), using the GTR model of sequence evolution.

To consider patterns in both loci simultaneously, each coral colony was assigned a genotype based on whether it had alleles from Clade A or B for *β-tub1* and Clade C or D from *b-tub2*. For example, a colony having two haplotypes from Clade A for *β-tub1* and one haplotype Clade C and one haplotype from Clade D for *β-tub2* would be assigned a genotype of AACD.

Results

Morphological analyses

Modern corals

Two morphotypes were recognized in the modern *thin section dataset* using cluster analysis (Figs. 4, 5): morphotype 1 (M1) consisting of 29 colonies and morphotype 2 (M2) consisting of 17 colonies. Both morphotypes consist of colonies collected in Belize, Panamá, Puerto Rico, and São Tomé. Canonical discriminant analysis based on the thin section dataset (46 colonies) shows that the two morphotypes are distinct (Wilks' Lambda = 0.206, $P < 0.001$; 97.8% correctly classified), and with one exception (colony ST254 from São Tomé, assigned to M1), they do not overlap. Pearson's correlations (Supplemental Table S5) between the original variables and the canonical variate (CV)

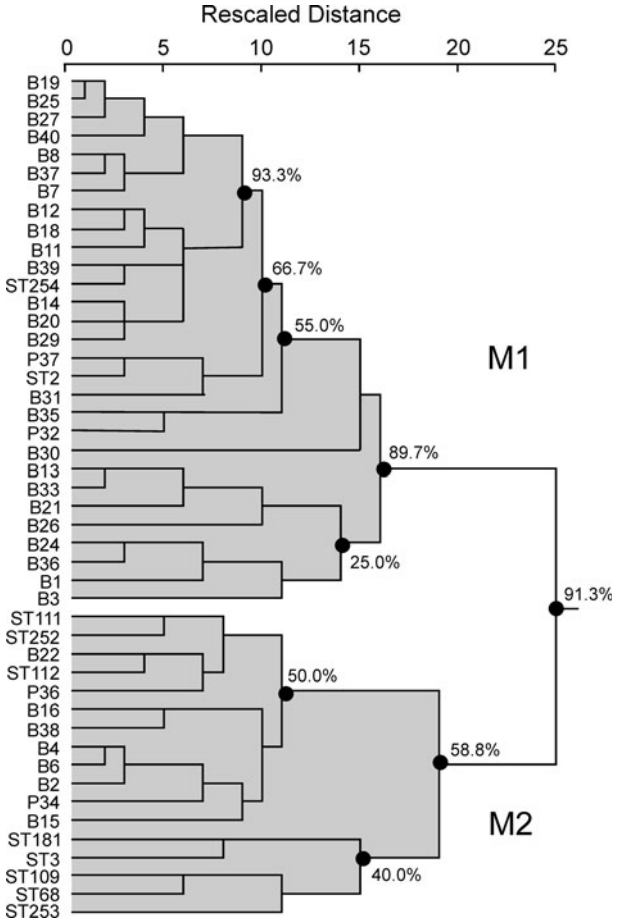

Fig. 4 Cluster analysis of *M. cavernosa* morphotypes based on Mahalanobis distances (F values) among colonies derived from the thin section dataset. Each branch represents one colony. Cross-validated classification results show that the branch agglomeration (=cluster) formed using the highest rescaled distance (morph 1 + morph 2) is 91.3% correctly classified; whereas the branch agglomeration formed using the second highest rescale distance (submorph c + d) is 58.8% correctly classified. Two morphotypes were therefore distinguished based on the highest agglomeration

indicate that centroid size (0.741) is most heavily weighted, followed by wall thickness (y11 = −0.227, y7 = −0.225) and tertiary septum length (y9 = 0.236, y17 = 0.199).

The canonical discriminant analysis based on the *calical surface dataset* (94 colonies) also shows that the two morphotypes are distinct (Wilks' Lambda = 0.474, $P < 0.001$; 86.9% correctly classified after non-thin-sectioned colonies were assigned to morphotype). Pearson's correlations between the original variables and the CV show that number of septa (NOSEPTA = 0.840) is most heavily weighted, followed by columella width (CW = 0.483) and corallite diameter (CD-MIN = 0.452, CD-AV = 0.407). Analysis of variance indicates that number of septa per corallite and corallite diameter are significantly higher in M1 than in M2 (Fig. 5).

Cross-tabulation results reveal a significant association between morphotype and locality for the 94 sampled colonies (Table 2); however, the association is not significant if

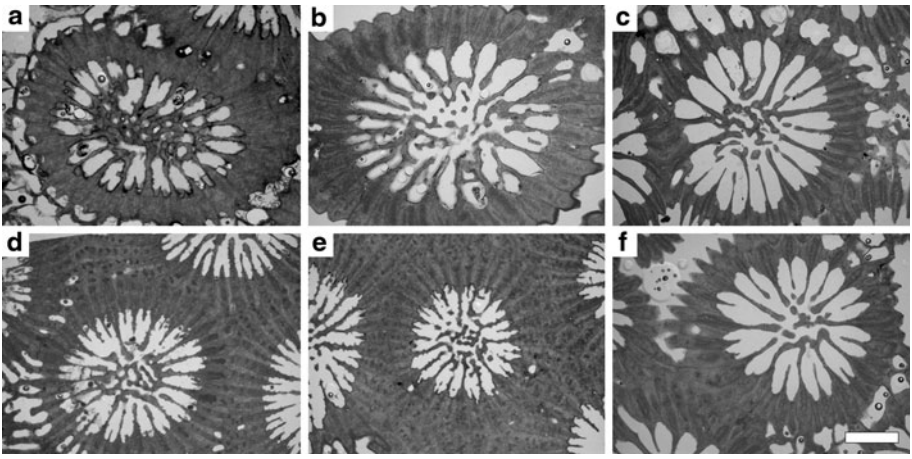

Fig. 5 Transverse thin sections of representative corallites of the two modern morphotypes (M1, M2). Oneway analysis of variance (*thin section dataset*) using $P < 0.05$ indicates that centroid size (csize), wall thickness (−y7, −y11, −y15), and tertiary septum length (y9, y17) are significantly higher in M1 than in M2. Oneway analysis of variance (*calical surface dataset*) indicates that corallite diameter (CD-MAX, CD-MIN, CD-AV), corallite shape (ROUNDNESS), columella width (CW), and number of septa (NOSEPTA) are significantly higher in M1 than M2. Corallite diameter averages 6.27 mm (±1.23) in M1 and 5.26 mm (±1.26) in M2; number of septa per corallite averages 43.9 (±4.0) in M1 and 32.5 (±9.17) in M2. Scale bar = 2 mm. **a** M1, Belize, E001, SUI 108547; **b** M1, Panamá, P032, SUI 125892; **c** M1, São Tomé, ST002, SUI 125898; **d** M2, Belize, E004, SUI 125923; **e** M2, Panamá, P036, SUI 125895; **f** M2, São Tomé, ST111, SUI 125905

the colonies from São Tomé are removed from the dataset (Chi-square = 0.740, $df = 2$, $P = 0.691$). No significant association was found between morphotype and water depth using the 32 colonies collected in Belize (Table 2). Tukey's results for the entire thin section dataset show that CV scores are lower overall for São Tomé and higher for Belize, with Panamá being intermediate and overlapping. However, Kruskal–Wallis tests for each morphotype show no differences in CV scores among localities within either morphotype. Neither Tukey's nor Kruskal–Wallis results reveal any significant differences in CV scores associated with water depth in Belize.

Fossil corals

Four morphotypes (Fig. 6) were recognized in the fossil dataset: F1 = 20 colonies, F2 = 12 colonies, F3 = 43 colonies, F4 = 3 colonies. Canonical discriminant analysis confirms that the four fossil morphotypes are distinct (Wilks' Lambda = 0.005, $P < 0.001$; 98.7% correctly classified; Supplemental Table S5), and with one exception (colony 46399 from Panamá, assigned to F3), they do not overlap. Scores on the first CV (inversely correlated with wall thickness) are low for F4, intermediate to low for F3, intermediate to high for F2, and high for F1, which each of the four morphotypes being significantly different. Scores on the second CV (correlated with septum length) are low for F2, and scores on the third CV (correlated with centroid size) are high for F4.

Combined canonical discriminant analyses of the four fossil and two modern morphotypes (Fig. 7; Supplemental Table S5) show that all six morphotypes are distinct (Wilks' Lambda = 0.042, $P < 0.001$; 89.5% correctly classified). Similarly, P values for F values based on Mahalanobis distances for all pairwise combinations of morphotypes are

Table 2 Crosstabulation results testing the association between morphotype and locality, and between morphotype and environment (water depth)

		Locality			Puerto Rico	Total
		Panamá	São Tomé	Belize		
Morphotype * locality crosstabulation (Chi-square = 33.141, $df = 3$, $P < 0.001$)						
Morpho-type	M1	4	4	31	19	58
	M2	2	22	8	4	36
Total		6	26	39	23	94

		Depth			Total
		<10 m	10–20 m	>20 m	
Morphotype * water depth crosstabulation (Chi-square = 0.235, $df = 2$, $P = 0.889$)					
Morpho-type	M1	5	12	8	25
	M2	2	3	2	7
Total		7	15	10	32

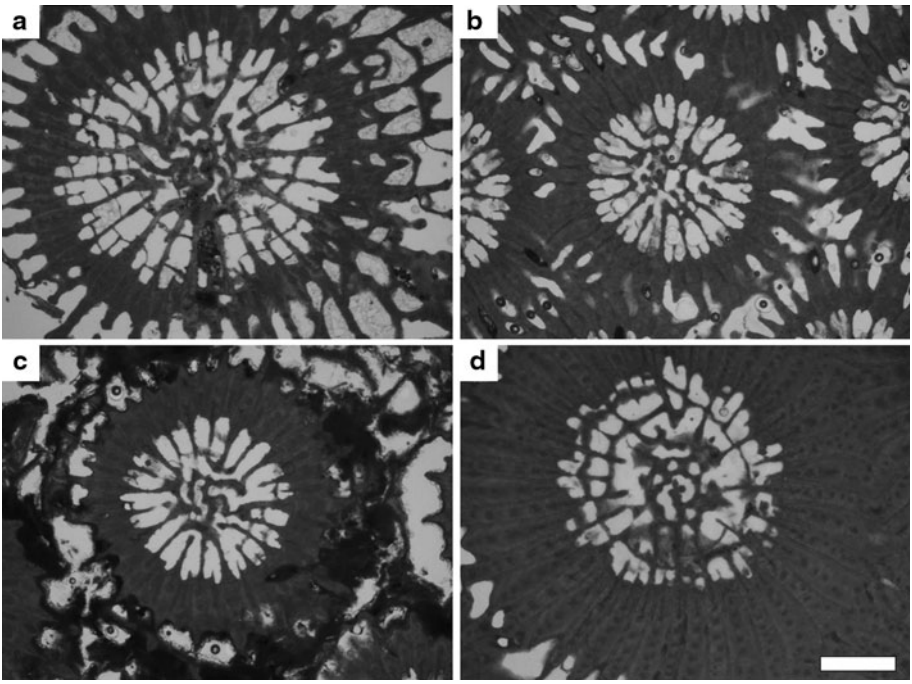

Fig. 6 Transverse thin sections of representative corallites of the four fossil morphotypes (F1–F4). Multiple comparisons tests (Table 1) indicate that wall thickness (−y7, −y11, −y15) is high in F4, intermediate in F3, and low in F1 and F2; tertiary septum length (y9, y17) is high in F1, high to intermediate in F2, low to intermediate in F3, and low in F4; corallite diameter (y1) is high in F1 and F4, low in F2, and overlapping in F3; centroid size is high in F4 and low in F1, F2, and F3. Scale bar = 2 mm. **a** F1, 493, Costa Rica, SUI 108459; **b** F2, PN311, Panamá, SUI 108511; **c** F3, 3220, Costa Rica, SUI 108479; **d** F4, PN307, Panamá, SUI 108507

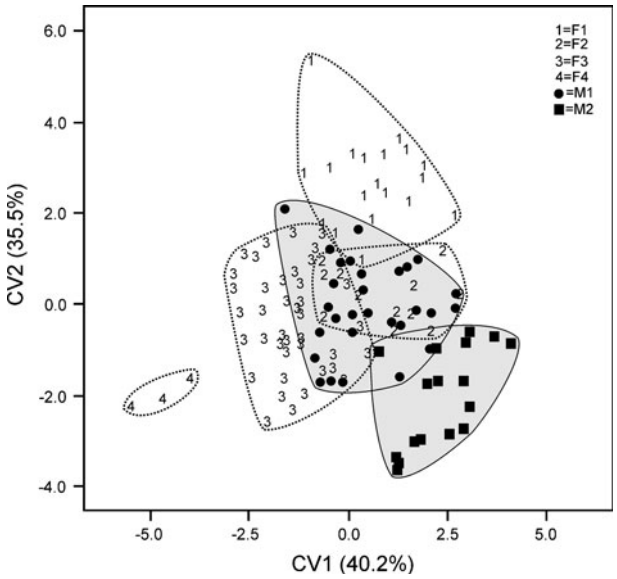

Fig. 7 Plots of scores on canonical variates (CV) comparing the 6 morphotypes (2 modern, 4 fossil). The analysis was performed using the thin section dataset. Each point on the plot represents one colony; *dotted* polygons enclose each fossil morphotype and *solid* polygons (*shaded*) enclose each modern morphotype. In legend, *M* modern; *F* fossil

Table 3 Mahalanobis distances between all pairwise combinations of fossil and modern morphotypes

Morphotype	F1	F2	F3	F4	M1
F2	15.130				
F3	13.744	12.138			
F4	52.864	48.499	18.362		
M1	**9.880**	13.783	**6.474**	34.993	
M2	25.978	15.438	17.253	53.024	**10.046**

Distances in bold are less than or equal to the distance between M1 and M2

all $P < 0.001$, indicating significant differences among morphotypes. However, the Mahalanobis distance value (Table 3) between the two modern morphotypes, M1 versus M2 (10.046) is greater than the distance between M1 versus F1 (9.880) and between M1 versus F3 (6.474). Moreover, the Mahalanobis distances for F2 versus F3 (12.138) and F2 versus M1 (13.783) are only slightly higher than the distance between M1 versus M2. The only fossil morphotype with high Mahalanobis distances between it and the other five species is F4, which consists of only three colonies.

Molecular analyses

After alignment and trimming, sequence lengths for *β-tub1* were 961 bp and for *β-tub2*, 612 bp. Among all sampled individuals, 59 haplotypes were observed for *β-tub1* and 29 haplotypes were observed for *β-tub2*. The two markers were tested for linkage

disequilibrium, and although linkage was detected among a subset of nucleotide sites within each locus, no significant linkage was found across the two markers (data not shown), implying that these two markers are independent loci. In addition, the absence of linkage indicates that no associations exist between alleles of the two loci. Haplotype networks for *β-tub1* (Fig. 8a) and *β-tub2* (Fig. 8b) show that both genes are composed of

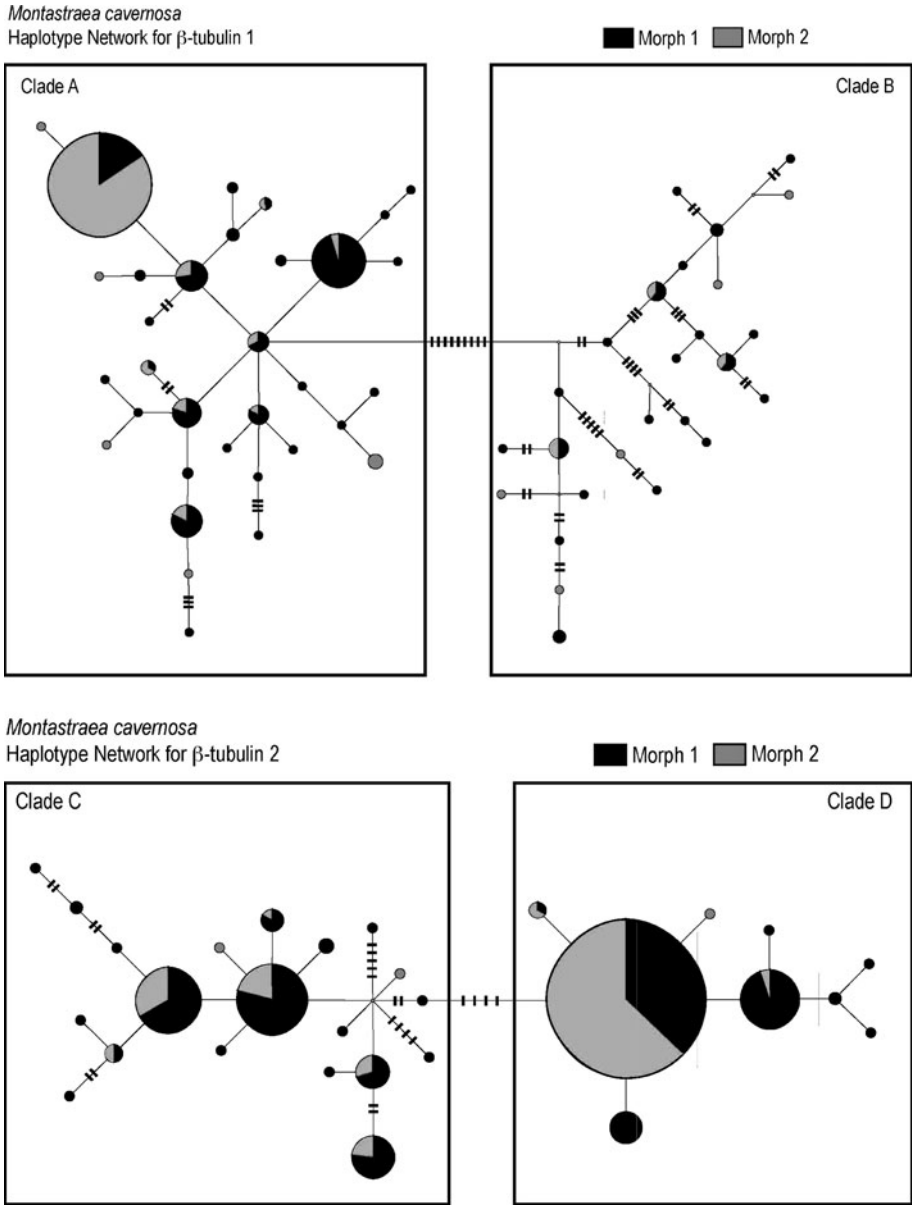

Fig. 8 Parsimony haplotype network for **a** *β-tub1* and **b** *β-tub2*. The size of each circle reflects the frequency that a haplotype is observed. Notches symbolize the number of mutations between haplotypes. Haplotypes observed in the morphotypes M1 and M2 are listed in *black* and *grey* respectively

two groups or 'clades' of haplotypes. For *β-tub1,* the clades have been named A and B, and for *β-tub2*, C and D. Both NJ and MP phylogenetic trees support these clade separations (Fig. S1), with bootstrap values of 97% for Clades A and B and 94% for Clade D (both NJ and MP). Haplotype L08, representing one haplotype in the Belize population, is not included in Clade C in either phylogenetic tree, but lies between the two clades (Fig. 8). All other haplotypes assigned to Clade C in the haplotype network form a cluster in the phylogenetic analyses, which has bootstrap support of 84 and 81% for NJ and MP respectively. For *β-tub1*, clades A and B have an average divergence of 1.71 ± 0.27%. For *β-tub2*, clades C and D have an average divergence of 1.51 ± 0.27%. The level of divergence between clades is greater than the average within-clade divergences, which are 0.47, 0.74, 0.64 and 0.40% for clades A, B, C and D, respectively (Fig. 9). To test whether these clades could potentially represent cryptic species, morphotypes identified using multivariate statistics (see above) were mapped onto the haplotype networks to determine if particular morphotypes could be correlated with specific haplotype clades. However, no association was detected between morphotypes and genetic clades in either *β-tub1* or *β-tub2* (Fig. 8).

An analysis of the genotypes occurring in each morphotype shows that all two-locus genotypes are found in both morphotypes (with the exception of the ABDD genotype

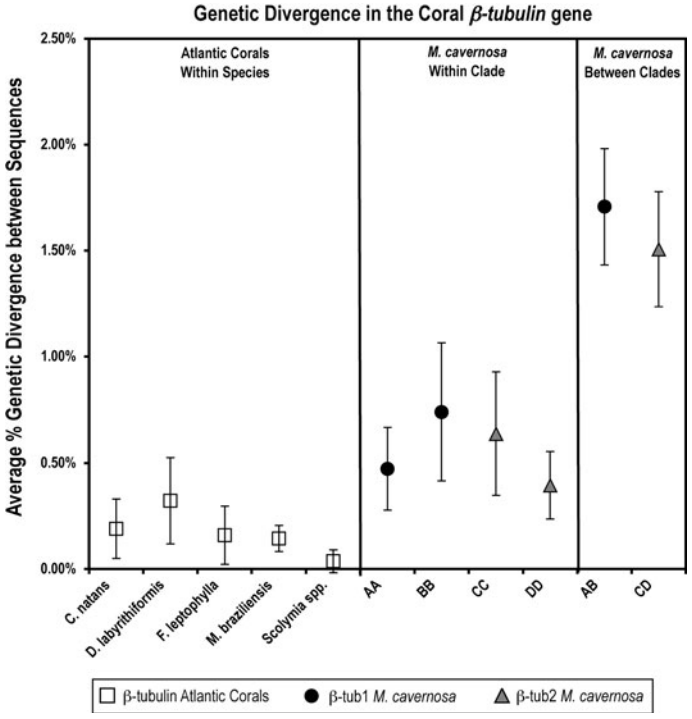

Fig. 9 Comparison of sequence divergence within and between haplotypes clades observed in *M. cavernosa* (this study), and intraspecific divergence observed in other Atlantic corals (Nunes et al. 2008). Open squares represent *β-tub* sequence data in Atlantic corals, *black circles* are *β-tub1* sequences in *M. cavernosa* and *grey triangles* are *β-tub2* sequences in *M. cavernosa*. The genetic divergence between haplotype clades in *M. cavernosa* is greater than is typically observed at this locus for other Atlantic coral species

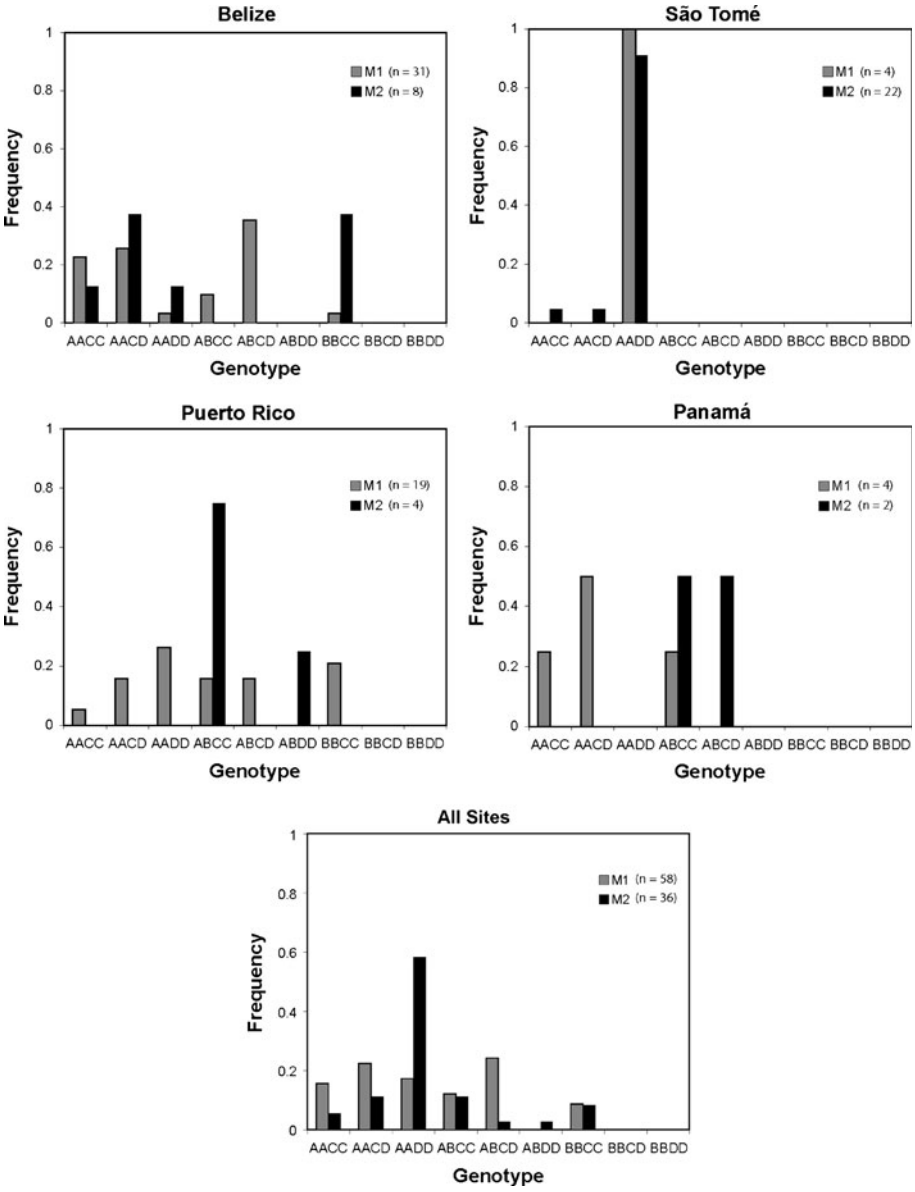

Fig. 10 Frequency of genotypes of *Montastraea cavernosa* from four localities in the Caribbean and West Africa

observed in 2% of morphotype M2) and that the frequency of genotypes is similar in the two morphotypes for each population (Fig. 10). In addition, 30.8% of colonies were heterozygous for Clades A and B, and 32.7% of colonies were heterozygous for Clades C and D. The expectation for a cryptic species would be that one group of individuals would have alleles from a given haplotype clade for each locus. Instead, it appears that alleles from

Table 4 Estimate of differentiation (φst) between morphological groups (M1 and M2) for each population

	M1 Belize	M1 Panama	M1 Puerto Rico	M1 São Tomé	M2 Belize	M2 Panama	M2 Puerto Rico	M2 São Tomé
M1 Belize		−0.025	0.005	**0.384**	−0.023	−0.095	−0.011	**0.411**
M1 Panama	−0.014		0.017	**0.528**	−0.059	−0.166	−0.09	**0.608**
M1 Puerto Rico	0.009	0.027		**0.374**	0.014	−0.03	−0.016	**0.416**
M1 São Tomé	**0.208**	**0.252**	**0.255**		**0.476**	**0.626**	**0.582**	−0.041
M2 Belize	0.015	0.028	−0.019	**0.295**		−0.104	−0.022	**0.533**
M2 Panama	0.007	0.056	−0.036	**0.516**	−0.059		−0.128	**0.651**
M2 Puerto Rico	0.039	0.096	0.004	**0.425**	0.005	−0.155		**0.642**
M2 São Tomé	**0.298**	**0.47**	**0.387**	−0.019	**0.501**	**0.732**	**0.651**	

Values in bold have *P* values below the significance level of $\alpha = 0.05$. In the lower triangle are values for *β-tub1* and in the upper triangle are values for *β-tub2*

each haplotype clade can be exchanged, and one third of the sampled colonies possess one allele from each clade for both loci.

Finally, a ϕst test was conducted to determine whether the two morphotypes were genetically differentiated. For each geographic population, two groups of haplotypes were defined based on morphotype (M1 and M2), and ϕst values were calculated for every pairwise combination of groups (Table 4). Most comparisons between morphotypes M1 and M2 do not have significant ϕst values. The only significant ϕst values were found between the São Tomé population and each of the three Caribbean populations. However, morphotypes M1 and M2 from São Tomé are not genetically differentiated, and have non-significant ϕst values.

Discussion

Cryptic species

We find no evidence for cryptic species in *Montastraea cavernosa*. Our results indicate polymorphism in both morphology and the *β-tub1* and *β-tub2* genes, but morphological and genetic polymorphism are not correlated. Two distinct morphotypes (Fig. 4), with M1 roughly corresponding to the nocturnal morph and M2 to the diurnal morph of Lasker (1976, 1979, 1980, 1981), and two haplotype clades per genetic locus (Fig. 8) were recognized. Morphotypes were distinguished using the same morphometric techniques as those used to distinguish the three species in the *Montastraea annularis* complex, and differences among *M. cavernosa* morphotypes are comparable to differences observed among *M. annularis* complex species (Pandolfi and Budd 2008). Moreover, Nunes et al. (2008) calculated an average intraspecific genetic divergence for the *β-tubulin* gene across five species of Atlantic corals (*Colpophyllia natans*, *Diploria labyrinthiformis*, *Favia leptophylla*, *Mussismilia braziliensis* and *Scolymia* sp) and found that the average genetic distance among haplotypes of the same species was $0.14 \pm 0.1\%$. In *M. cavernosa*, the genetic divergences between Clades A and B ($1.51 \pm 0.27\%$) for *β-tub1* and Clades C and D for *β-tub2* ($1.51 \pm 0.27\%$) are an order of magnitude higher than the within-clade divergences and intra-specific divergence observed for other species (Fig. 9).

Nevertheless, maps of morphotypes onto haplotype networks (Fig. 8) show that morphotypes and haplotype clades do not correspond. They also show no evidence of linkage disequilibrium between the two loci, indicating no associations between alleles that would be indicative of cryptic species. Moreover, ϕst tests show that genetic differentiation is not significant between morphotypes (Table 4). Finally, the two morphotypes of *M. cavernosa* do not differ in genotype frequencies (Fig. 10). Approximately one third of the sampled colonies were heterozygous for Clades A and B, or Clades C and D, suggesting that genes can be exchanged across haplotype clades. The lack of correspondence between morphology and genetics contrasts numerous studies on reef corals over the past decade, which have found concordance between these two data types (e.g., Fukami et al. 2004a; Flot et al. 2008; Forsman et al. 2009), and is similar to the growth forms observed in *Platygyra daedalea*, which cannot be explained by genetic or environmental data (Miller and Benzie 1997).

Comparisons between genotype frequencies in *M. cavernosa* (Fig. 10) and the *M. annularis* complex (Fukami et al. 2004a) indicate more genetic overlap between *M. cavernosa* morphotypes than between species in the *M. annularis* complex. In the *M. annularis* complex in Panamá, *M. faveolata* has almost no shared genotypes with *M. franksi* and *M. annularis*, and *M. annularis* and *M. franksi* differ in frequencies of genotypes AAA and AA*. In *M. cavernosa* (Fig. 10), both morphotypes share nearly all of the same genotypes, with the exception of the relatively rare genotype ABDD, which is only observed in morphotype M2. The two morphotypes do differ overall in genotype frequency, with the AADD genotype being more frequently observed in M2. However, this is likely caused by AADD being the dominant genotype in São Tomé (22 of 26 colonies) and nearly all individuals in São Tomé being M2 (24 of 26 colonies). The São Tomé population is geographically and genetically isolated from the three Caribbean populations, which would allow genotype frequencies to diverge via stochastic processes such as genetic drift.

Geographic and environmental variation

Our results show no evidence for either geographic or environmental variation within *Montastraea cavernosa*. With regard to geographic variation, the segregation of genotypes, morphotypes or both to specific geographical locations is expected if divergence is the result of allopatric speciation. Several marine cryptic species have been identified on the basis of high genetic divergence between specimens from different geographic locations; for example, the blenny *Ophioblennius atlanticus* (Muss et al. 2001) and the sponge *Chondrilla nucula* (Klautau et al. 1999). In *M. cavernosa*, however, haplotypes from all four clades in *β-tub1* and *β-tub2* occur at all of the sampled sites. In addition, both morphotypes occur at similar frequencies in all localities in the Caribbean. The São Tomé population is an exception, being dominated by the M2 morphotype and AADD genotype (Table 2). However, the AADD genotype and M2 morphotype are both commonly found in all other populations, and are not necessarily associated in the Caribbean or São Tomé populations (not all M2 morphotypes have an AADD genotype and vice versa).

With regard to environmental variation, specifically phenotypic plasticity (recently reviewed by Todd 2008), both morphotypes co-occur at all water depths in Belize, and no significant differences were found in morphology among colonies collected in different water depths (but see Ruiz 2004). Together these two results suggest that phenotypic plasticity is not solely responsible for the observed morphological differences between morphotypes. Moreover, they contrast with the results of morphological analyses on the

Montastraea annularis complex collected from exactly the same reef sites in Belize, in which costa length was found to be associated with water depth in *M. annularis* and *M. faveolata* and shape of the tertiary costa with water depth in *M. franksi* (Pandolfi and Budd 2008). Klaus et al. (2007) examined the relationships between light, δ15 N (sewage indicator), δ13C (autotrophy: heterotrophy), *Symbiodinium* communities, and morphology in *M. annularis* s.s. collected over a water depth gradient in Curaçao, and observed changes in calical elevation. These authors concluded that morphological differences between colonies collected in environments characterized by extreme differences in water energy, sedimentation rate, and nutrient supply may be caused by phenotypic plasticity. However, plasticity plays less of a role within a single environment or across a subtle environmental gradient. The fact that each of the two *M. cavernosa* morphotypes occur in the same environment suggests that genetic factors (e.g., related to calcification and/or development) are at least partly responsible for their morphological differences.

High levels of polymorphism in *Montastraea cavernosa*

Unlike most other eukaryotes, the coral mitochondrial genome is highly conserved (Shearer et al. 2002; Hellberg 2006), but higher genetic variation is increasingly being found in the coral nuclear genome (e.g., Baums et al. 2005; Eytan et al. 2009). Comparisons between nuclear and mitochondrial datasets suggest that coral nuclear loci are 2–10 times more variable than mitochondrial loci (Chen et al. 2009; Eytan et al. 2009); however, few studies have estimated how much variation is typical of coral nuclear genes. The genetic variation observed in *β-tub1* and *β-tub2* of *Montastraea cavernosa* is higher than previously reported. As many as 74 haplotypes of the *β-tub1* gene have been identified in *M. cavernosa* (Nunes et al. 2009), and intra-specific sequence divergence observed in the present study is as high as 2.55%. This level of intra-specific variation has rarely been observed in corals, with the exception of the ribosomal internal transcribed spacer (ITS) regions (e.g., Diekmannn et al. 2001 in *Madracis*; Forsman et al. 2005 in *Siderastrea*; Rodriguez-Lanetty and Hoegh-Guldberg 2002 in *Plesiastrea*; Wei et al. 2006 in *Acropora*), but the high number of gene copies and greater intra- than inter-specific variation found in this locus (Vollmer and Palumbi 2004) complicates phylogenetic inference.

A comparative study across several trans-Atlantic coral species suggests that variation in the *β-tubulin* gene of *M. cavernosa* may be greater than that of several other corals (Nunes 2009). In this locus, *M. cavernosa* has much greater variation compared to brooders such as *Favia fragum*, *Favia gravida*, *Porites astreoides* and *Siderastrea radians*. The broadcasting gonochoric species *S. siderea* has greater variation at the *β-tubulin* gene than the above-mentioned brooders, but its variation is lower than that observed for *M. cavernosa* (Nunes 2009).

A combination of factors may explain why *M. cavernosa* is able to maintain high levels of genetic diversity compared to other coral species. First, the expected polymorphism at mutation-drift equilibrium is predicted to be proportional to the effective population size (Gillespie 2004). Thus, organisms with high effective population sizes should have high genetic diversity. *M. cavernosa* is a common coral species with a wide distribution across the Atlantic, both of which are indicative of a large population size, and by extension, high genetic diversity. Second, small, fragmented populations are more susceptible to loss of diversity via genetic drift (Gillespie 2004). *M. cavernosa* is able to maintain high genetic connectivity throughout the Caribbean and along the coast of Brazil (Nunes et al. 2009), which may contribute to its ability to maintain high genetic variation compared to coral species with fragmented populations such as *Acropora* spp (Baums et al. 2005; Vollmer

and Palumbi 2007), *M. faveolata* (Severance and Karl 2006) and *Favia* spp (Nunes 2009; Goodbody-Gringley et al. 2010). Third, reproductive strategies may also affect levels of genetic diversity. It has been argued that gonochorism may evolve under selection for increased outcrossing and greater rates of recombination (Szmant 1986). Gonochorism may therefore favor high genetic diversity in *M. cavernosa.* Simultaneous hermaphrodites, such as the members of the *M. annularis* complex, are largely self-incompatible (Levitan et al. 2004) and are therefore likely to have similar rates of outcrossing. Self-compatible hermaphrodites, on the other hand, are expected to suffer from reduced genetic diversity, as has been observed for corals that are capable of self-fertilization such as *F. fragum* and *P. astreoides* (Brazeau et al. 1998).

Long-term evolutionary implications

Our study shows that the magnitude of variation exhibited by the modern and fossil morphotypes is roughly equivalent, with the possible exception of F4, a morphotype that is difficult to assess due to low sample size (Fig. 7; Table 3). Given the lack of genetic differentiation found among modern morphotypes, by extrapolation, we can interpret the four fossil morphotypes as representing one polymorphic species, which is the same as modern *Montastraea cavernosa.* Moreover, based on the observed morphological overlap between modern and fossil specimens (Fig. 7), with the Mahalanobis distances between M1 and F3 and between M1 and F1 being less than the distance between M1 and M2 (Table 3), this one highly variable species can be interpreted as exhibiting no net evolutionary change from first to last occurrence, or in other words, "morphological stasis" (Hunt 2007).

Using traditional linear distance measurements, Budd (1991) recognized four *M. cavernosa*-like morphospecies with >36 septa per corallite in the Mio-Pliocene of the Dominican Republic (Table 5). Visual comparisons of the four fossil morphotypes in the present study with these four Dominican Republic morphospecies indicate that F1 corresponds with *M. cavernosa*, F2 with *M. canalis*, and F3 with *M. cylindrica*; F4 does not match any of the Dominican Republic species. Three of the Dominican Republic morphospecies (*M. canalis*, *M. cavernosa,* and *M. cylindrica*) may therefore be synonymous with modern *M. cavernosa* and represent different polymorphs of *M. cavernosa*. More rigorous quantitative morphological data need to be analyzed to verify these assignments.

Table 5 Four *M. cavernosa*-like morphospecies with >36 septa per corallite in the Mio-Pliocene of the Dominican Republic (after Budd 1991), and their diagnostic characteristics

Previously reported fossil morphospecies	Corallite diameter (mm)	Number of septa per corallite	Corallite spacing (mm)	Costae	First occurrence (Johnson 2001, 2007; Johnson and Kirby 2006)
M. canalis (Vaughan 1919)	4.5–5.5	36–42	5.9–6.6	Equal	Late Oligocene Antigua Formation of Antigua (~26–25 Ma)
M. cylindrica (Duncan 1863)	4–5	24–36	9–11	Thin unequal	Early to middle Miocene Tamana Formation of Trinidad (~16.4–12.3 Ma)
M. endothecata (Duncan 1863)	7.2–9	36–50	<9	Thick unequal	Late Oligocene Antigua Formation of Antigua (~26–25 Ma)
M. cavernosa (Linnaeus 1767)	5.5–6.5	38–48	5.9–6.6	Unequal	Late Oligocene Antigua Formation of Antigua (~26–25 Ma)

Study of first occurrence data whose age dates are based primarily on microfossils (Table 5) indicates that *M. cavernosa* (including the above proposed synonyms) has a divergence time of at least ~26–25 Ma, and thus a total species duration of >25 myr, an amount far longer than most modern Caribbean reef coral species, which have originated within the past 5 myr (Budd and Johnson 1999). In view of the lack of correlation between morphological and genetic data reported above, it seems unlikely that the individual fossil morphotypes of *M. cavernosa* represent species lineages that can be traced through geologic time. Instead they may represent polymorphs that repeatedly develop within each of the sampled time intervals. The difficulty in tracing morphotypes through time is exemplified by the geometric morphometric study of Schultz and Budd (2008), who found a bewildering array of eight overlapping morphotypes of *M. cavernosa* in the Neogene of the Dominican Republic, which could not unequivocally be linked to morphotypes in fossil units outside of the Dominican Republic (in part due to sample size). Two of the 8 morphotypes appear to correspond with *M. endothecata*, one with *M. canalis*, one with *M. cylindrica*, one with *M. cavernosa*, and the remaining three were interpreted as new.

Further evidence supporting polymorphism in the fossil record can be drawn from co-occurrence data for the three synonymous morphospecies (*M. canalis*, *M. cavernosa,* and *M. cylindrica*), which indicate that even during the Miocene and Pliocene they co-occur in the same localities. Johnson (2001) reports co-occurrences of *M. canalis* and *M. cylindrica* in the early to middle Miocene of Trinidad. In the Dominican Republic (Budd et al. 1994; Klaus et al. 2008), *M. canalis* and *M. cavernosa* co-occur in the late Miocene Cercado Formation (~6.5–5.6 Ma), *M. canalis*, *M. cavernosa,* and *M. cylindrica* co-occur in the Gurabo Formation (~5.6–4.5 Ma), and *M. canalis, M. cylindrica* and *M. cavernosa* co-occur in the Mao Formation ~4.5–3.5 Ma). In the present study, all four morphotypes occur in both formations, and often in the same locality; e.g., F1–F4 at locality AB95-08 ("corales overkill") and F1–F3 at locality CJ92-6 ("Lomas del Mar – e") in Costa Rica, and F1–F3 at both AB99-10 ("Wild Cane Key") and CM06-10 ("Minitimbi") in Panamá.

Caveats

Montastraea cavernosa exhibits high morphological and genetic variation, but high polymorphism is not associated with cryptic species. The patterns observed in the present study should be taken with caution, however, because the data involve only two nuclear loci. Although these two nuclear loci show no evidence of linkage disequilibrium (Nunes et al. 2009), they are duplications of the same gene and may not be entirely independent of one another. These two genes may not be representative of the genome as a whole, and additional genetic data could reveal patterns that are not observed in *β-tub1* and *β-tub2*. Reproductive data provided by cross-fertilization experiments between gametes of the two morphotypes are also needed to further test for cryptic species.

Similarly, morphological data in the present study focus on two-dimensional traits in transverse thin section, which are associated with overall corallite size (centroid size) and the structure of the corallite wall. In addition to three-dimensional calical morphology, data for soft-tissue and colony-level features (e.g., colony size) would provide a more complete morphological characterization of the two modern morphotypes. Although phenotypic plasticity may not be responsible for the observed morphological differences, our understanding of how environment affects skeletal growth and corallite architecture in *M. cavernosa* is limited. Field and aquarium transplantation experiments, which use clonemates, assess symbiont activity, and accurately monitor a broad range of environmental

parameters, are needed to detect within-genotype plastic responses, and tease apart the effects of genetics, symbionts, and environment on morphological variation.

Conclusion

Our results show that polymorphism in *Montastraea cavernosa* is maintained in the presence of gene flow, is widespread across the geographic range of the species, and may have existed for 25 myr of geologic time, including the severe environmental perturbations of the Plio-Pleistocene. Phenotypic plasticity is poorly understood in the species, but does not explain the observed patterns. More information about ecological and reproductive differences between the two modern morphotypes, as well as diagnostic genetic markers and analyses tracing morphotypes through geologic time, are needed to unravel the complex cause of polymorphism and its genetic basis. Nevertheless, the observed high levels of gene flow, large population size, and reduced rates of speciation in the gonochoric species, *M. cavernosa*, contrast observations in many hermaphroditic reef corals, and may be responsible for its unusually long duration and apparent morphological stasis.

Acknowledgments We thank Myra Laird (University of Iowa) and Jonathan Lee (University of California, San Diego) for photography and measuring specimens, and Matthew Wortel (University of Iowa Geoscience Petrographic Facilities) for preparing thin sections. Diving assistance in Belize was provided by Claudia and Dan Miller. David Anderson assisted with specimen collection and morphological measurements in Puerto Rico. Nancy Knowlton and Richard Norris provided helpful comments and discussions. This research was supported by a grant from the US National Science Foundation Grant [DEB-0343208 to AFB], a doctoral fellowship from the Center of Marine Biodiversity and Conservation [to FN], the John Dove Isaacs Chair in Natural Philosophy [to N. Knowlton], the Department of Marine Sciences, University of Puerto Rico [to EW], and both the Australian Research Council Centre of Excellence for Coral Reef Studies and the Smithsonian Institution's Marine Science Network grants [to JMP].

References

Acosta A, Zea S (1997) Sexual reproduction of the reef coral *Montastrea cavernosa* (Scleractinia: Faviidae) in the Santa Marta area, Caribbean coast of Colombia. Mar Biol 128:141–148

Barroso R, Klautau M, Sole-Cava AM, Paiva PC (2010) Eurythoe complanata (Polychaeta: Amphinomidae), the 'cosmopolitan' fireworm, consists of at least three cryptic species. Mar Biol 157:69–80

Baums IB, Miller MW, Hellberg ME (2005) Regionally isolated populations of an imperiled Caribbean coral, *Acropora palmata*. Mol Ecol 14:1377–1390

Bookstein FL (1991) Morphometric tools for landmark data. Cambridge University Press, Cambridge 435 p

Brazeau DA, Gleason DF, Morgan ME (1998) Self-fertilization in brooding hermaphroditic Caribbean corals: evidence from molecular markers. J Exp Mar Biol Ecol 231:225–238

Budd AF (1991) Neogene Paleontology in the Northern Dominican Republic. 11. The Family Faviidae (Anthozoa: Scleractinia). Part I. Bull AmPaleontol 101(338):5–83, pls. 1–29

Budd AF (1993) Variation within and among morphospecies of *Montastraea*. Courier Forschungs-institut Senckenberg 164:241–254

Budd AF, Johnson KG (1999) Origination preceding extinction during Late Cenozoic turnover of Caribbean reefs. Paleobiology 25:188–200

Budd AF, Klaus JS (2001) The origin and early evolution of the *Montastraea "annularis"* species complex (Anthozoa: Scleractinia). J Paleontol 75:527–545

Budd AF, Klaus JS (2008) Early evolution of the *Montastraea "annularis"* species complex (Anthozoa: Scleractinia): Evidence from the Mio-Pliocene of the Dominican Republic. In: Nehm RH, Budd AF (eds) Evolutionary stasis and change in the Dominican Republic Neogene. Springer, New York, pp 85–124

Budd AF, Pandolfi JM (2004) Overlapping species boundaries and hybridization within the *Montastraea "annularis"* reef coral complex in the Pleistocene of the Bahama Islands. Paleobiology 30:396–425

Budd AF, Pandolfi JM (2010) Evolutionary novelty is concentrated at the edge of species distributions. Science 328:1558–1561

Budd AF, Stemann TA, Stewart RH (1992) Eocene Caribbean reef corals: a unique fauna from the Gatuncillo Formation of Panama. J Paleontol 66:570–594

Budd AF, Stemann TA, Johnson KG (1994) Stratigraphic distributions of genera and species of Neogene to Recent Caribbean reef corals. J Paleontol 68:951–977

Budd AF, Johnson KG, Stemann TA, Tompkins BH (1999) Pliocene to Pleistocene reef coral assemblages in the Limon Group of Costa Rica. In: Collins LS, Coates AG (eds), A Paleobiotic Survey of the Caribbean Faunas from the Neogene of the Isthmus of Panama. Bulletins of American Paleontology, Special Volume 357:119–158

Calvo M, Templado J, Oliverio M, Machordom A (2009) Hidden Mediterranean biodiversity: molecular evidence for a cryptic species complex within the reef building vermetid gastropod Dendropoma petraeum (Mollusca: Caenogastropoda). Biol J Linn Soc 96:898–912

Carpenter KE and 38 others (2008) One-third of reef building corals face elevated extinction risk from climate change and local impacts. Science 321:560–563

Chen IP, Tang CY, Chiou CY et al (2009) Comparative analyses of coding and noncoding DNA regions indicate that Acropora (Anthozoa: Scleractina) possesses a similar evolutionary tempo of nuclear vs. mitochondrial genomes as in plants. Mar Biotechnol 11:141–152

Clement M, Posada D, Crandall KA (2000) TCS: a computer program to estimate gene genealogies. Mol Ecol 9:1657–1659

Coates AG, McNeill DF, Aubry M-P, Berggren WA, Collins LS (2005) An introduction to the geology of the Bocas del Toro Archipelago, Panama. Caribb J Sci 41:374–391

Collins LS, Coates AG (eds) (1999) A Paleobiotic Survey of Caribbean Faunas from the Neogene of the Isthmus of Panama. Bull Am Paleontol 357:351

Diekmannn OE, Bak RPM, Stam WT, Olsen JL (2001) Molecular genetic evidence for probable reticulate speciation in the coral genus *Madracis* from a Caribbean fringing reef slope. Mar Biol 139:221–233

Duncan PM (1863) On the fossil corals of the West Indian Islands. Part 1. Q J Geol Soc Lond 20:406–458, pls 13–16

Eldredge N, Gould SJ (1972) Punctuated equilibria: an alternative to phyletic gradualism. In: Schopf TJM (ed) Models in paleobiology. Freeman Cooper, San Francisco, pp 82–115

Excoffier L, Laval G, Schneider S (2005) Arlequin ver. 3.0: an integrated software package for population genetics data analysis. Evolutionary Bioinformatics Online 1

Eytan RI, Hayes M, Arbour-Reily P, Miller M, Hellberg ME (2009) Nuclear sequences reveal mid-range isolation of an imperilled deep-water coral population. Mol Ecol 18:2375–2389

Flot J, Magalon H, Cruard C, Couloux A, Tillier S (2008) Patterns of genetic structure among Hawaiian corals of the genus Pocillopora yield clusters of individuals that are compatible with morphology. Comptes Rendus Biol 331:239–247

Forsman ZH, Guzman HM, Chen CA, Fox GE, Wellington GM (2005) An ITS region phylogeny of *Siderastrea* (Cnidaria:Anthozoa): is *S. glynni* endangered or introduced? Coral Reefs 24:343–347

Forsman ZH, Barshis DJ, Hunter CL, Toonen RJ (2009) Shape-shifting corals: molecular markers show morphology is evolutionarily plastic in Porites. BMC Evol Biol 9:45

Fukami H, Budd AF, Levitan DR, Jara J, Kersanach R, Knowlton N (2004a) Geographic differences in species boundaries among members of the *Montastraea annularis* complex based on molecular and morphological markers. Evolution 58:324–337

Fukami H, Budd AF, Paulay G, Solé-Cava A, Chen CA, Iwao K, Knowlton N (2004b) Conventional Taxonomy Obscures Deep Divergence between Pacific and Atlantic Corals. Nature 427:832–835

Fukami H, Chen CA, Budd AF, Collins A, Wallace C, Chuang Y-Y, Chen C, Dai C-F, Iwao K, Sheppard C, Knowlton N (2008) Mitochondrial and nuclear genes suggest that stony corals are monophyletic but most families of stony corals are not (Order Scleractinia, Class Anthozoa, Phylum Cnidaria). PLoS One 3(9):e3222(1–9)

Gillespie JH (2004) Population genetics: a concise guide, 2nd edn. The Johns Hopkins University Press, Baltimore 232 pp

Goodbody-Gringley G, Vollmer SV, Woollacott RM, Giribet G (2010) Limited gene flow in the brooding coral *Favia fragum* (Esper, 1797). Marine Biology. doi:10.1007/s00227-00010-01521-00226

Goreau TF (1959) The ecology of Jamaican coral reefs. I. Species composition and zonation. Ecology 40:67–90

Goreau TF, Wells JW (1967) The shallow-water Scleractinia of Jamaica: revised list of species and their vertical distribution range. Bull Mar Sci 17:442–453

Hellberg ME (2006) No variation and low synonymous substitution rates in coral mtDNA despite high nuclear variation. BMC Evol Biol 6:24

Hunt G (2007) The relative importance of directional change, random walks, and stasis in the evolution of fossil lineages. Proc Natl Acad Sci 104:18404–18408

Jablonski D (2007) Scale and hierarchy in macroevolution. Palaeontology 50:87–109

Jackson JBC, Cheetham AH (1990) Evolutionary significance of morphospecies; a test with cheilostome Bryozoa. Science 248:579–583

Jackson JBC, Cheetham AH (1999) Tempo and mode of speciation in the sea. Trends Ecol Evol 14:72–77

Johnson KG (2001) Middle Miocene recovery of Caribbean reef corals: new data from the Tamana Formation of Trinidad. J Paleontol 75:513–526

Johnson KG (2007) Reef-coral diversity in the Late Oligocene Antigua Formation and temporal variation of local diversity on Caribbean Cenozoic Reefs. In: Hubmann B, Piller WE (eds) Fossil Corals and Sponges. Proceedings of the 9th International Symposium on Fossil Cnidaria and Porifera. Österr. Akad. Wiss., Schriftenr. Erdwiss. Komm. 17:471–491, 1 Tab., 5 Figs., 2 Pls., Wien

Johnson KG, Kirby MX (2006) The Emperador Limestone rediscovered: Early Miocene corals from the Culebra Formation, Panama. J Paleontol 80:283–293

Klaus JS, Budd AF, Heikoop JM, Fouke BW (2007) Environmental controls on corallite morphology in the reef coral *Montastraea annularis*. Bull Mar Sci 80:233–260

Klaus JS, Budd AF, Johnson KG, McNeill DF (2008) Assessing community change in Miocene to Pliocene coral assemblages of the northern Dominican Republic. In: Nehm RH, Budd AF (eds) Evolutionary stasis and change in the Dominican Republic Neogene. Springer, New York, pp 193–224

Klautau M, Russo CAM, Lazoski C et al (1999) Does cosmopolitanism result from overconservative systematics? A case study using the marine sponge Chondrilla nucula. Evolution 53:1414–1422

Knowlton N (1993) Sibling species in the sea. Ann Rev Ecol Syst 24:189–216

Knowlton N (2000) Molecular genetic analyses of species boundaries in the sea. Hydrobiologica 420:73–90

Knowlton N, Budd AF (2001) Recognizing coral species past and present. In: Jackson JBC, Lidgard S, McKinney FK (eds) Evolutionary patterns: growth, form, and tempo in the fossil record. Univ. Chicago Press, Chicago, pp 97–119

Knowlton N, Jackson JBC (1994) New taxonomy and niche partitioning on coral reefs: jack of all trades or master of some? Trends Ecol Evol 9:7–9

Knolwton N, Weil E, Weigt LA, Guzman HM (1992) Sibling species in *Montastraea annularis*, coral bleaching, and the coral climate record. Science 255:330–333

Laborel J (1969) Madréporaires et Hydrocoralliaires récifaux des côtes brésiliiennes. Annales del Institute Océanographique 47:171–229, 8 pls

Laborel J (1974) West African reefs corals: an hypothesis on their origin. Proceedings of the 2nd International Coral Reef Symposium 1: 425–443

Lasker HR (1976) Intraspecific variability of zooplankton feeding in the hermatypic coral *Montastraea cavernosa*. In: Mackie GW (ed) Coelenterate ecology and behavoir. Plenum Press, New York, pp 101–109

Lasker HR (1979) Light dependent activity patterns among reef corals: *Montastraea cavernosa*. Biol Bull 156:196–211

Lasker HR (1980) Sediment rejection by reef corals: the roles of behavior and morphology in *Montastraea cavernosa* (Linnaeus). J Exp Mar Biol Ecol 47:77–87

Lasker HR (1981) Phenotypic variation in the coral *Montastraea cavernosa* and its effects on colony energetics. Biol Bull 160:292–302

Lee T, Foighil DO (2005) Placing the Floridian marine genetic disjunction into a regional evolutionary context using the scorched mussel, Brachidontes exustus, species complex. Evolution 59:2139–2158

Levitan DR, Fukami H, Jara J, Kline D, McGovern TM, McGhee KE, Swanson CA, Knowlton N (2004) Mechanisms of reproductive isolation among sympatric broadcast-spawning corals of the *Montastraea annularis* species complex. Evolution 58:308–323

Lin HC, Sanchez-Ortiz C, Hastings PA (2009) Colour variation is incongruent with mitochondrial lineages: cryptic speciation and subsequent diversification in a Gulf of California reef fish (Teleostei: Blennioidei). Mol Ecol 18:2476–2488

Linneaus C (1767) Madrepora. Systema Naturae, Holmiae, Editio Duodecima, Reformata, t.1, pt.2, pp 1272–1282

Mathews LM (2006) Cryptic biodiversity and phylogeographical patterns in a snapping shrimp species complex. Mol Ecol 15:4049–4063

McNeill DF, Coates AG, Budd AF, Borne PF (2000) Integrated paleontologic and paleomagnetic stratigraphy of the upper Neogene deposits around Limon, Costa Rica: a coastal emergence record of the Central American Isthmus. Geol Soc Am Bull 112:963–981

Miller KJ, Benzie JAH (1997) No clear genetic distinction between morphological species within the coral genus *Platygyra*. Bull Mar Sci 61:907–917

Muss A, Robertson DR, Stepien CA, Wirtz P, Bowen BW (2001) Phylogeography of Ophioblennius: the role of ocean currents and geography in reef fish evolution. Evolution 55:561–572

Nunes F (2009) Biodiversity and connectivity in peripheral populations of corals of the South and Eastern Atlantic. PhD Dissertation, University of California, San Diego, 142 pp

Nunes F, Fukami H, Vollmer SV, Norris RD, Knowlton N (2008) Re-evaluation of the systematics of the endemic corals of Brazil by molecular data. Coral Reefs 27:423–432

Nunes F, Norris RD, Knowlton N (2009) Implications of isolation and low genetic diversity in peripheral populations of an amphi-Atlantic coral. Mol Ecol 18:4283–4297

Pandolfi JM, Budd AF (2008) Morphology and ecological zonation of Caribbean reef corals: the *Montastraea 'annularis'* species complex. Mar Ecol Prog Ser 369:89–102

Rodriguez-Lanetty M, Hoegh-Guldberg O (2002) The phylogeography and connectivity of the latitudinally widespread scleractinian coral *Plesiastrea versipora* in the Western Pacific. Mol Ecol 11:1177–1189

Ruiz H (2004). Morphometric examination of corallite and colony variability in the Caribbean coral *Montastraea cavernosa* (Linnaeus 1766). Ms.C Thesis (Advisor Dr. Ernesto Weil). Department of Marine Sciences, University of Puerto Rico Mayaguez, 79 pp

Schultz HA, Budd AF (2008) Neogene evolution of the reef coral species complex *Montastraea "cavernosa"*. In: Nehm RH, Budd AF (eds) Evolutionary stasis and change in the Dominican Republic Neogene. Springer, New York, pp 147–170

Severance EG, Karl SA (2006) Contrasting population genetic structures of sympatric, mass-spawning Caribbean corals. Mar Biol 150:57–68

Shearer TL, Van Oppen MJH, Romano SL, Worheide G (2002) Slow mitochondrial DNA sequence evolution in the Anthozoa (Cnidaria). Mol Ecol 11:2475–2487

Slatkin M (1987) Gene flow and the geographic structure of natural populations. Science 236:787–792

Stephens M, Scheet P (2005) Accounting for decay of linkage disequilibrium in haplotype inference and missing-data imputation. Am J Hum Genet 76:449–462

Stephens M, Smith NJ, Donnelly P (2001) A new statistical method for haplotype reconstruction from population data. Am J Hum Genet 68:978–989

Sterrer W (ed) (1986) Marine fauna and flora of Bermuda. Wiley, New York 774 pp

Szmant AM (1986) Reproductive ecology of Caribbean Reef Corals. Coral Reefs 5:43–53

Szmant AM (1991) Sexual reproduction by the Caribbean reef corals *Montastraea annularis* and *M. cavernosa*. Mar Ecol Prog Ser 74:13–25

Szmant AM, Weil E, Miller MW, Colon DE (1996) Hybridization in the species complex of *Montastraea annularis*. Mar Biol 129:561–572

Tamura K, Dudley J, Nei M, Kumar S (2007) MEGA4: Molecular evolutionary genetics analysis (MEGA) software version 4.0. Mol Biol Evol 24:1596–1599

Thompson JD, Gibson TJ, Plewniak F, Jeanmougin F, Higgins DG (1997) The CLUSTAL_X windows interface: flexible strategies for multiple sequence alignment aided by quality analysis tools. Nucleic Acids Res 25:4876–4882

Todd PA (2008) Morphological plasticity in scleractinian corals. Biol Rev 83:315–337

Vaughan TW (1919) Fossil corals from Central America, Cuba, and Porto Rico with an account of the American Tertiary, Pleistocene, and recent coral reefs. U.S. National Museum Bulletin 103:189–524, pls. 68–152

Vollmer SV, Palumbi SR (2004) Testing the utility of internally transcribed spacer sequences in coral phylogenetics. Mol Ecol 13:2763–2772

Vollmer SV, Palumbi SR (2007) Restricted gene flow in the Caribbean staghorn coral *Acropora cervicornis*: Implications for the recovery of endangered reefs. J Hered 98:40–50

Wei NV, Wallace CC, Dai CF, Pillay RM, Chen CA (2006) Analyses of the Ribosomal Internal Transcribed Spacers (ITS) and the 5.8S Gene Indicate that Extremely High rDNA Heterogeneity is a Unique Feature in the Scleractinian Cora Genus *Acropora* (Scleractinia;Acroporidae). Zool Stud 45(3):404–418

Weil E, Knowlton N (1994) A multi-character analysis of the Caribbean coral *Montastraea annularis* (Ellis & Solander, 1786) and its two sibling species, *M. faveolata* (Ellis & Solander, 1786), and *M. franksi* (Gregory, 1895). Bull Mar Sci 54(3):151–175

Xia X, Xie Z (2001) DAMBE: software package for data analysis in molecular biology and evolution. J Hered 92:371–373

Zelditch ML, Swiderski DL, Sheets HD, Finks WL (2004) Geometric morphometrics for biologists: a primer. Elsevier, Amsterdam, 416 p